

A Composite Linear and Nonlinear Approach to Full-Vehicle Simulator Control

Mark J. Brudnak

U.S. Army RDECOM-TARDEC

ABSTRACT

This paper presents an approach to full-vehicle simulator control which accounts for nonlinearities in a vehicle/simulator system. The control scheme presented is based on the estimation of the system inverse dynamics. A composite linear/nonlinear approach to inverse system identification (SYS-ID) is presented. The linear portion of the SYS-ID uses time-domain methods to estimate the impulse response of the inverse system in a least squares sense. These results are then extended by using the regularized approach to least squares estimation. The nonlinear part uses the support vector machine to approximate the nonlinear deviations from the linear model. Two approaches to using this composite model are presented. Examples of the linear SYS-ID techniques are shown for a 2x2 system.

INTRODUCTION

With an ever increasing emphasis on vehicle reliability both in the military and automotive industry, the science of simulation and laboratory testing has correspondingly developed. To gain confidence that a particular vehicle will endure its expected service environment, durability tests are performed prior to production and fielding. The time and cost of such tests has motivated the development of laboratory based full vehicle test rigs (FVTR) which have displaced much of the time-consuming proving ground durability tests.

These FVTRs were initially tire-coupled and over time evolved into multi-axial spindle-coupled configurations which are able to impose multiple forces at each spindle. Along with the development of the hardware has been a corresponding development of the control strategies used to simulate actual road inputs. The earliest methods used road profile information, "effective road profiles" [10], or a stationary random process to simulate road roughness. These methods used, to some degree or another, the concept of the road profile as a conceptual arbitrator between the test rig command input and the on-vehicle response. Then Cryer, Nawrocki and Lund [5] removed the conceptual necessity of the road profile, by modeling the relationship between the command input and the on-vehicle response as a

frequency response function (FRF). They then showed how this FRF could be used to estimate the proper simulator command, given a desired on-vehicle response. Their method became the foundation of the industry standard approach to simulator drive determination.

Although this linear FRF-based approach has been the industry standard for nearly three decades, it has difficulty compensating for nonlinearities inherently present in automotive systems. To overcome system nonlinearities, FRF-based methods use an iterative process to converge on the proper drive command. As the techniques have been applied to increasingly complex road simulators, they have been extended to the non-square case by Fash, Goode and Brown [6], and have incorporated singular value decomposition techniques to handle ill-conditioned FRFs, but they have still remained dependent on the linear mathematics of the FRF model.

This paper presents an approach to drive command development which incorporates both linear and nonlinear modeling methods to directly learn the inverse dynamics of the simulator/vehicle combination. First, it describes the problem of drive development in practical and historical terms. Then, it discusses the mathematics and algorithms of the existing approaches and their associated limitations. It formally states the problem of drive command development in mathematical terms and gives the rationale behind the composite model. It then discusses alternative approaches to both the linear and nonlinear modeling and justifies the particular choices made. Finally, it presents some proposed alternatives for drive command correction. The paper concludes with some examples.

BACKGROUND

The fundamental problem of full-vehicle simulation is that of replication of the service environment. The service environment is typically approximated by a drive cycle on a set of courses at a proving ground. At the proving ground vibrational excitation comes from a terrain profile represented by $p(x)$ (where $x(t)$ is the distance down the course as a function of time) which creates

Report Documentation Page

Form Approved
OMB No. 0704-0188

Public reporting burden for the collection of information is estimated to average 1 hour per response, including the time for reviewing instructions, searching existing data sources, gathering and maintaining the data needed, and completing and reviewing the collection of information. Send comments regarding this burden estimate or any other aspect of this collection of information, including suggestions for reducing this burden, to Washington Headquarters Services, Directorate for Information Operations and Reports, 1215 Jefferson Davis Highway, Suite 1204, Arlington VA 22202-4302. Respondents should be aware that notwithstanding any other provision of law, no person shall be subject to a penalty for failing to comply with a collection of information if it does not display a currently valid OMB control number.

1. REPORT DATE 10 JAN 2005	2. REPORT TYPE N/A	3. DATES COVERED -	
4. TITLE AND SUBTITLE A Composite Linear and Nonlinear Approach to Full-Vehicle Simulator Control		5a. CONTRACT NUMBER	
		5b. GRANT NUMBER	
		5c. PROGRAM ELEMENT NUMBER	
6. AUTHOR(S) Mark J. Brudnak		5d. PROJECT NUMBER	
		5e. TASK NUMBER	
		5f. WORK UNIT NUMBER	
7. PERFORMING ORGANIZATION NAME(S) AND ADDRESS(ES) USA TACOM 6501 E 11 Mile Road Warren, MI 48397-5000		8. PERFORMING ORGANIZATION REPORT NUMBER 14118	
9. SPONSORING/MONITORING AGENCY NAME(S) AND ADDRESS(ES)		10. SPONSOR/MONITOR'S ACRONYM(S) TACOM TARDEC	
		11. SPONSOR/MONITOR'S REPORT NUMBER(S)	
12. DISTRIBUTION/AVAILABILITY STATEMENT Approved for public release, distribution unlimited			
13. SUPPLEMENTARY NOTES U.S. Government Work; not copyrighted in the U.S. Presented at SAE World Congress 2005, The original document contains color images.			
14. ABSTRACT			
15. SUBJECT TERMS			
16. SECURITY CLASSIFICATION OF:			17. LIMITATION OF ABSTRACT SAR
a. REPORT unclassified	b. ABSTRACT unclassified	c. THIS PAGE unclassified	
			18. NUMBER OF PAGES 12
			19a. NAME OF RESPONSIBLE PERSON

acceleration responses $a_i(t)$ at the spindles of the vehicle under test (as shown in Figure 1). On a full-vehicle simulator the command inputs $c_i(t)$ directly affect the actuator displacements $d_i(t)$, which in turn affect the acceleration responses $\tilde{a}_i(t)$ at the spindles of the vehicle under test (as shown in Figure 2). The standard of validity for full vehicle simulation is that the rig responses $\tilde{a}_i(t)$ approximately match those recorded at the proving ground $a_i(t)$, which is mathematically stated as

$$\tilde{a}_i(t) \approx a_i(t), \quad \forall i = 1, \dots, n. \quad (1)$$

Now the determination of the simulator command $c_i(t)$ which assures that this is the case is called *drive command development*.

Prior to the work of Cryer et al., drive file development focused on the measurement and replication of the terrain profile $p(x)$. The drive command was then derived from the profile as

$$c_i(t) = f_{p,i}(p(x_i(t)))$$

for some distance function $x_i(t)$. The function $f_{p,i}(\cdot)$ is then used to assure that (1) holds. The dependence on the profile $p(x)$ is the fundamental limitation of this approach.

The innovation of Cryer et al. was to directly replicate $a_i(t)$ (called the *desired response*) by defining the drive command $c_i(t)$ as being solely dependent on the set $\{a_i(t)\}_{i=1}^n$ as

$$c_i(t) = f_{c,i}(a_1(\tau_t), \dots, a_n(\tau_t)) \quad (2)$$

where the interval $\tau_t \triangleq (t - t_{\text{up}}, t - t_{\text{low}})$ denotes a dynamic relationship between the desired response $\{a_i(t)\}_{i=1}^n$ and $c_i(t)$. Let the simulator be governed by the dynamics

$$\tilde{a}_i(t) = f_{a,i}(c_1(\zeta_t), \dots, c_n(\zeta_t)) \quad (3)$$

for $\zeta_t = (-\infty, t)$. Equations (2) and (3) may then be vectorized as

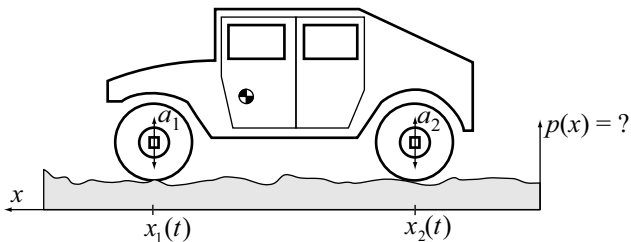


Figure 1. Field environment to be replicated.

$$\begin{aligned} \tilde{\mathbf{a}}(t) &= \mathbf{f}_a(\mathbf{c}(\zeta_t)) \\ \mathbf{c}(t) &= \mathbf{f}_c(\mathbf{a}(\tau_t)) \end{aligned} \quad (4)$$

where $\tilde{\mathbf{a}}(t) = [\tilde{a}_1(t) \dots \tilde{a}_n(t)]^T$, $\mathbf{a}(t) = [a_1(t) \dots a_n(t)]^T$, and $\mathbf{c}(t) = [c_1(t) \dots c_n(t)]^T$ are $n \times 1$ column vectors (i.e. \mathbb{R}^n) by convention. Cryer et al. then regard the system as a black box relationship between its inputs and outputs without regard to the unnecessary concept of the terrain profile. Their method will be elaborated in the "EXISTING METHODS" section.

CONTROL PROBLEM – Given the definitions in (4), the function $\mathbf{f}_c(\cdot)$ must be defined so that $\tilde{\mathbf{a}}(t)$ tracks the desired response $\mathbf{a}(t)$. Cast in these terms, the determination of the proper $\mathbf{f}_c(\cdot)$ is a control problem. Traditionally this control problem has been solved by attempting to guarantee that

$$\mathbf{a}(t) \approx \tilde{\mathbf{a}}(t) = \mathbf{f}_a \circ \mathbf{f}_c(\mathbf{a}(t))$$

and solving for $\mathbf{f}_c(\cdot)$ yields

$$\mathbf{f}_c(\cdot) = \mathbf{f}_a^{-1}(\cdot). \quad (5)$$

If $\mathbf{f}_a(\cdot)$ is perfectly known and is invertible everywhere over its range then (5) assures that (1) will hold. Now given that $\mathbf{f}_a(\cdot)$ consists of the dynamics of vehicle specimen, the simulator, and the PID controller, it is not readily derivable from first principles. Additionally, $\mathbf{f}_a(\cdot)$ is typically not known down a finite number of unknown physical parameters due to the presence of the unmodeled vehicle dynamics. Worse still $\mathbf{f}_a(\cdot)$ is nonlinear. Given these circumstances, existing practice is to perform a system identification on the plant (vehicle and simulator) to obtain the estimated system dynamics $\hat{\mathbf{f}}_a(\cdot)$. The following section briefly describes the method of Cryer et al. in the determination of $\mathbf{f}_c(\cdot)$.

EXISTING METHODS – The methods developed by Cryer et al. are based on discrete-time, linear math in the frequency-domain. Let the input and output signals

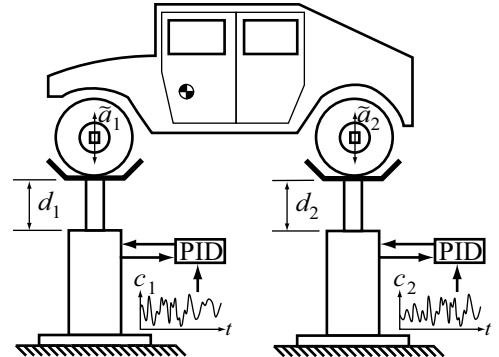


Figure 2. Simulator with HMMVV attached.

($c_i(t)$ and $a_i(t)$ respectively) be discretized at a sample time T_s such that $t = kT_s$. Also let the inputs and outputs be transformed into the frequency-domain as $\tilde{\mathbf{a}}(f_j) = \mathcal{F}\{\tilde{\mathbf{a}}(k)\}$ and $\mathbf{c}(f_j) = \mathcal{F}\{\mathbf{c}(k)\}$ where $\mathcal{F}\{\cdot\}$ denotes the discrete Fourier transform (DFT). Cryer et al. then define $\mathbf{f}_a(\cdot)$ as

$$\tilde{\mathbf{a}}(k) = \mathbf{f}_a(\mathbf{c}(\zeta_k)) \triangleq \mathbf{H}(\cdot) * \mathbf{c}(k) \quad (6)$$

where $\mathbf{H}(k)$ is the system *impulse response function* and $*$ denotes the convolution operation. Equation (6) has the corresponding frequency-domain representation

$$\tilde{\mathbf{a}}(f_j) = \mathbf{H}(f_j)\mathbf{c}(f_j)$$

where $\mathbf{H}(f_j)$ is the system FRF. Since $\mathbf{H}(f_j)$ is not known, it must be experimentally determined, so let $\mathbf{n}(k)$ be a suitable colored-noise signal used to excite the simulator, obtaining the response $\mathbf{r}(k)$. If $\mathbf{n}(k)$ and $\mathbf{r}(k)$ have DFTs $\mathbf{n}(f_j)$ and $\mathbf{r}(f_j)$ respectively, then the frequency response function is estimated as

$$\hat{\mathbf{H}}(f_j) = \mathbf{S}_{\mathbf{r}\mathbf{n}}(f_j)\mathbf{S}_{\mathbf{n}\mathbf{n}}^{-1}(f_j)$$

where $\mathbf{S}_{\mathbf{n}\mathbf{n}}(f_j) = \mathbb{E}[\mathbf{n}(f_j)\mathbf{n}^H(f_j)]$ is the *auto-spectral density* (ASD) of $\mathbf{n}(k)$ and $\mathbf{S}_{\mathbf{r}\mathbf{n}}(f_j) = \mathbb{E}[\mathbf{r}(f_j)\mathbf{n}^H(f_j)]$ is the *cross-spectral density* (CSD) of $\mathbf{r}(k)$ and $\mathbf{n}(k)$. Now according to (5), $\hat{\mathbf{H}}(f_j)$ must be inverted to obtain the estimated drive $\hat{\mathbf{c}}(k)$ from $\mathbf{a}(k)$, thus yielding

$$\hat{\mathbf{c}}(k) = \mathbf{f}_c(\mathbf{a}(k)) \triangleq \hat{\mathbf{H}}^{\text{inv}}(\cdot) * \mathbf{a}(k)$$

where $\hat{\mathbf{H}}^{\text{inv}}(k) = \mathcal{F}^{-1}\{\hat{\mathbf{H}}^{-1}(f_j)\}$. In the frequency-domain the drive command estimate is

$$\hat{\mathbf{c}}(f_j) = \hat{\mathbf{H}}^{-1}(f_j)\mathbf{a}(f_j)$$

which is independent for each frequency line f_j .

Now because $\hat{\mathbf{H}}(k)$ is a linear estimate of a nonlinear system, $\hat{\mathbf{c}}(k)$ will not be optimal. To obtain the best drive estimate the *iteration* process is used. Let the initial drive estimate be defined as $\hat{\mathbf{c}}_0(k) = \mathbf{w}_0 \circ (\hat{\mathbf{H}}^{\text{inv}}(\cdot) * \mathbf{a}(k))$

where $\mathbf{w}_0 \in [0,1]^n$ is a weight vector and \circ denotes an element-wise product. Then $\hat{\mathbf{c}}_0(k)$ is used to drive the simulator and the corresponding response $\tilde{\mathbf{a}}_0(k)$ is recorded. Let $\mathbf{e}_0(k) = \mathbf{a}(k) - \tilde{\mathbf{a}}_0(k)$ denote error between the desired response and actual response, then the drive estimate correction is given by $\hat{\mathbf{c}}_1(k) = \hat{\mathbf{c}}_0(k) + \mathbf{w}_1 \circ (\hat{\mathbf{H}}^{\text{inv}}(\cdot) * \mathbf{e}_0(k))$. This process is repeated according to the rule

$$\hat{\mathbf{c}}_{i+1}(k) = \hat{\mathbf{c}}_i(k) + \mathbf{w}_{i+1} \circ (\hat{\mathbf{H}}^{\text{inv}}(\cdot) * \mathbf{e}_i(k)) \quad (7)$$

and progress is measured by monitoring a statistic of the error which is typically

$$\mathbf{m}_i = \frac{\text{RMS}_k(\mathbf{e}_i(\cdot))}{\text{RMS}_k(\mathbf{a}(\cdot))} \quad (8)$$

where $\text{RMS}_k(\cdot): \mathbb{R}^{n \times \ell} \mapsto \mathbb{R}^n$ and division is computed element-wise. This iterative process is terminated when each element of \mathbf{m}_i is sufficiently small.

In practice this iterative process requires 10 to 20 such iterations to obtain satisfactory convergence. It is widely known that the success of the iteration process is dependent on

1. The quality of the forward model $\hat{\mathbf{H}}(k)$.
2. The choice of excitation $\mathbf{n}(k)$.
3. The choice of the weights \mathbf{w}_i .
4. The stationarity of the desired response $\mathbf{a}(k)$.

Each of these issues can cause difficulty in obtaining sufficiently small relative errors \mathbf{m}_i and make the process highly dependent on the skills of the practitioner. It is believed that most of these difficulties originate from the essential nonlinear nature of the plant. Thus to obtain effective improvement in drive file development, we claim that the nonlinearities of the plant must be incorporated into the inverse model $\mathbf{f}_c(\cdot)$. It is this goal that motivates the approach presented in the sequel.

PROBLEM DEFINITION AND APPROACH

Since the forward dynamics of the plant $\mathbf{f}_a(\cdot)$ are nonlinear, the inverse $\mathbf{f}_c(\cdot)$ will also be nonlinear.

However since the linear model $\hat{\mathbf{H}}^{\text{inv}}(k)$ is used to yield a first order approximation of the inverse, it is clear that it contains significant information about the plant dynamics. Therefore, the linear model will be retained here and a nonlinear modeling approach will be used to approximate the deviations from the linear model. This approach is illustrated in Figure 3 where the forward dynamics are modeled as

$$\mathbf{f}_a(\mathbf{c}(k)) = \mathbf{H}(\cdot) * \mathbf{c}(k) + \boldsymbol{\omega}(\mathbf{c}(\kappa_k)) \quad (9)$$

and the inverse dynamics are modeled by

$$\mathbf{f}_c(\mathbf{a}(k)) = \mathbf{H}^{\text{inv}}(\cdot) * \mathbf{a}(k) + \boldsymbol{\psi}(\mathbf{a}(\kappa_k)) \quad (10)$$

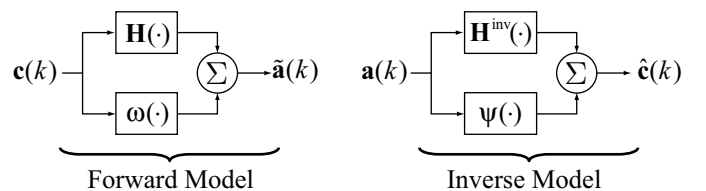


Figure 3. Linear/Nonlinear approach to modeling.

where in each case $\kappa_k \triangleq \{k - k_{\max}, \dots, k - k_{\min}\}$ is an index set for $\mathbf{c}(\cdot)$ or $\mathbf{a}(\cdot)$. The concept behind this approach is illustrated in Figure 4. As can be seen, the

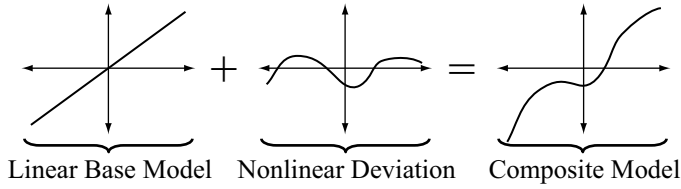


Figure 4. Illustration of composite model.

linear model provides a global base-model and the nonlinear part is only concerned with the small deviations from the base model. This approach may be divided into the modeling problem and the control problem as follows.

Modeling Problem: Given a set of recorded inputs $\mathbf{n}(k)$ and outputs $\mathbf{r}(k)$ assembled into the training set $\{\{\mathbf{n}(k), \mathbf{r}(k)\}\}_{i=1}^{\ell}$, find $\hat{\mathbf{H}}^{\text{inv}}(k)$ and $\hat{\psi}(\cdot)$ such that

$$\mathbf{n}(k) \approx \hat{\mathbf{H}}^{\text{inv}}(\cdot) * \mathbf{r}(k) + \hat{\psi}(\mathbf{r}(\kappa_k))$$

and there is a high expectation that such an inverse model will provide a good estimate of the proper command $\mathbf{c}(\cdot)$ given the desired response $\mathbf{a}(\cdot)$.

Control Problem: Once obtained, how should the inverse model (10) be used to find the proper command input? This assumes that the initial estimate of the inverse model will not be sufficiently accurate to generate the best estimate of the drive command.

MODELING CHOICES

This section begins the discussion of the modeling approach. In the determination of $\mathbf{H}^{\text{inv}}(k)$ and $\psi(\cdot)$ many alternatives exist for both the linear and nonlinear parts. Generally, these choices are as follows.

PARAMETRIC VS. NONPARAMETRIC MODEL – The first and most important choice is whether to make use of prior information (if any exists) about the plant. If explicit equations for the dynamics of the system are known down to a few unknown physical parameters, then it is generally preferable to use these equations to identify the system. This is called the *parametric* approach. On the other hand, if the system's governing equations are not known, then a "Black Box" approach is needed to model the system. Unfortunately, this is almost always the case so the black box (or *nonparametric*) approach will be used here.

FORWARD VS. INVERSE IDENTIFICATION – The second choice is whether to identify the forward pair $\mathbf{H}(\cdot)$ and $\omega(\cdot)$ from (9) and then algebraically invert

them as $\mathbf{H}^{\text{inv}}(f_j) = (\mathbf{H}(f_j))^{-1}$ and $\psi(\cdot) = \Psi\{\mathbf{H}(\cdot), \omega(\cdot)\}(\cdot)$ (this is usually called the *explicit/indirect* approach) or to identify the inverse models $\mathbf{H}^{\text{inv}}(\cdot)$ and $\psi(\cdot)$ in (10) directly (this is usually called the *implicit/direct* approach). As described above, the traditional linear method of Cryer et al. uses the explicit/indirect approach since the inversion of a linear operator is well understood. In the nonlinear case, the inversion of these models is much more difficult and is usually impossible. The approach pursued here will be the implicit/direct where $\mathbf{H}^{\text{inv}}(\cdot)$ and $\psi(\cdot)$ are estimated directly.

TIME- VS. FREQUENCY- DOMAIN – The last choice is whether to maintain the traditional frequency-domain approach to estimating the linear model $\mathbf{H}^{\text{inv}}(\cdot)$. It is well known that linear time-domain methods are just as suitable to the calculation of $\mathbf{H}^{\text{inv}}(\cdot)$. It is helpful to observe that the traditional methods were based on frequency-domain mathematics partly to take advantage of the efficiency of the fast Fourier transform (FFT). With the exponentially increasing power of the microprocessor, this motivation is not as pressing. Furthermore there are advantages to estimating $\mathbf{H}^{\text{inv}}(\cdot)$ in the time-domain which will be elaborated on in the following sections.

LINEAR MODELING

It may be shown that in the time-domain the forward model $\mathbf{H}(k) = \mathcal{F}^{-1}\{\mathbf{H}(f_j)\}$ is a causal FIR filter where $[\mathbf{H}(k)]_{ij} = h_{ij}(k)$ represents a matrix of impulse response functions $h_{ij}(k)$ for $k = 0, \dots, k_{\max}$ as shown in Figure 5. It may also be shown that $\mathbf{H}(k)$ has a stable causal inverse $\mathbf{H}^{\text{inv}}(k)$ if it is *minimum-phase*. If it is *mixed phase*, then a causal inverse is unstable, however it may be shown that an acausal inverse is stable. Therefore we may approximate $\mathbf{H}^{\text{inv}}(k)$ as an acausal FIR filter where $k = k_{\min}, \dots, 0, \dots, k_{\max}$ and $r \triangleq k_{\max} - k_{\min} + 1$ as illustrated in Figure 6. The inverse linear model then takes the form

$$\mathbf{c}_{\text{lin}}(k) = \mathbf{H}^{\text{inv}}(\cdot) * \mathbf{a}(k) \triangleq \sum_{i=k_{\min}}^{k_{\max}} \mathbf{H}^{\text{inv}}(i) \mathbf{a}(k-i). \quad (11)$$

For computational reasons, $\mathbf{H}^{\text{inv}}(\cdot)$ (which is triple-indexed or a *three-way array*) will be re-indexed as $\mathbb{R}^{n \times nr} \ni \mathbf{H}^{\text{inv}} \equiv \{\mathbf{H}^{\text{inv}}(k)\}_{k=k_{\min}}^{k_{\max}}$ where the column and time dimensions are combined in the new index $\lambda \triangleq \{1, \dots, nr\}$ which has a one-one correspondence to

the set of ordered pairs $\{(i, j)\}_{i,j=1}^{n,r} \leftrightarrow \lambda$. This “flattened” version then takes the form

$$\underline{\mathbf{H}}^{\text{inv}} \triangleq \begin{bmatrix} \mathbf{h}_{11}^{\text{inv}T} & \dots & \mathbf{h}_{1n}^{\text{inv}T} \\ \vdots & \ddots & \vdots \\ \mathbf{h}_{n1}^{\text{inv}T} & \dots & \mathbf{h}_{nn}^{\text{inv}T} \end{bmatrix}$$

where $\mathbf{h}_{ij}^{\text{inv}T} \triangleq [h_{ij}^{\text{inv}}(k_{\min}) \dots h_{ij}^{\text{inv}}(k_{\max})]$ is the inverse impulse response between $\tilde{a}_j(k)$ and $c_{\text{lin}_i}(k)$. Let $\mathbb{R}^{nr} \ni \underline{\boldsymbol{\phi}}_{\mathbf{a}}(k) \equiv \{\mathbf{a}(k-\eta)\}_{\eta=k_{\min}}^{k_{\max}}$ which is indexed by λ and

given by $\underline{\boldsymbol{\phi}}_{\mathbf{a}}(k) \triangleq [\mathbf{a}^T(k-k_{\min}) \dots \mathbf{a}^T(k-k_{\max})]^T$. Equation (11) may then be expressed as a matrix product

$$\mathbf{c}_{\text{lin}}(k) = \underline{\mathbf{H}}^{\text{inv}} \underline{\boldsymbol{\phi}}_{\mathbf{a}}(k) \quad (12)$$

and will be used as a basis for estimating $\mathbf{H}^{\text{inv}}(k)$ in the following section.

LEAST SQUARES METHOD – Now as stated earlier, the system is excited with colored noise $\mathbf{n}(k)$ and the response $\mathbf{r}(k)$ for $k=1, \dots, \ell$ is recorded. Then for each $\mathbf{r}(k)$ we form the regression vector $\underline{\boldsymbol{\phi}}_{\mathbf{r}}(k)$ using the index λ where clearly $\mathbf{r}(k) \triangleq \mathbf{0}$ for $k < 1$ and $k > \ell$. By hypothesis, the inverse plant model obeys (12) for any set of inputs and outputs which yields the transposed relation

$$\mathbf{n}^T(k) = \underline{\boldsymbol{\phi}}_{\mathbf{r}}^T(k) \underline{\mathbf{H}}^{\text{inv}T}.$$

Let $\mathbf{N} \triangleq [\mathbf{n}(1) \dots \mathbf{n}(\ell)]^T \in \mathbb{R}^{\ell \times n}$ and

$\underline{\boldsymbol{\Phi}}_{\mathbf{r}} \triangleq [\underline{\boldsymbol{\phi}}_{\mathbf{r}}(1) \dots \underline{\boldsymbol{\phi}}_{\mathbf{r}}(\ell)]^T \in \mathbb{R}^{\ell \times nr}$; then the following aggregated model is obtained

$$\mathbf{N} = \underline{\boldsymbol{\Phi}}_{\mathbf{r}} \underline{\mathbf{H}}^{\text{inv}T}.$$

The Moore-Penrose pseudo-inverse may be used to

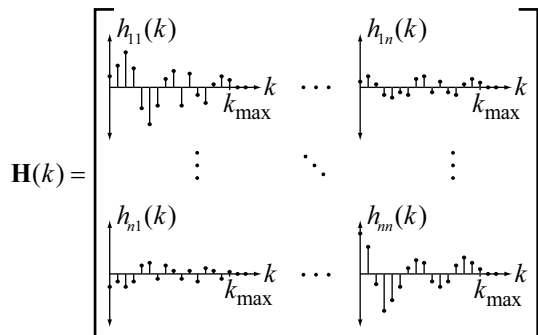


Figure 5. Forward Impulse Response.

solve for $\underline{\mathbf{H}}^{\text{inv}}$ as

$$\hat{\underline{\mathbf{H}}}^{\text{inv}T} = (\underline{\boldsymbol{\Phi}}_{\mathbf{r}}^T \underline{\boldsymbol{\Phi}}_{\mathbf{r}})^{-1} \underline{\boldsymbol{\Phi}}_{\mathbf{r}}^T \mathbf{N} \quad (13)$$

which may be shown to minimize the summed loss

$$\mathcal{J}(\underline{\mathbf{H}}^{\text{inv}}) \triangleq \frac{1}{2} \sum_{k=1}^{\ell} \|\mathbf{n}(k) - \underline{\mathbf{H}}^{\text{inv}} \underline{\boldsymbol{\phi}}_{\mathbf{r}}(k)\|_2^2 \quad (14)$$

and hopefully the expected loss

$$\mathbb{E} \left[\|\mathbf{n}(k) - \underline{\mathbf{H}}^{\text{inv}} \underline{\boldsymbol{\phi}}_{\mathbf{r}}(k)\|_2^2 \right]. \quad (15)$$

REGULARIZED LEAST SQUARES METHOD – Now $\underline{\mathbf{H}}^{\text{inv}}$ as learned using the least squares method is a non-parametric estimate with $n^2 r$ free parameters. Generally the half-length of the impulse response $\max(|k_{\min}|, |k_{\max}|)$ is chosen to correspond roughly to the settling time of the system. So for a small sample time T_s and long settling time we typically have $k_{\max} \sim 100$ which means that $\underline{\mathbf{H}}^{\text{inv}}$ will have hundreds if not thousands of free parameters. This is typically more than the number of degrees of freedom n_d in the actual system. Therefore an ideal model would only contain n_d degrees of freedom. Unfortunately, n_d is not known but it may be asserted with confidence that $n^2 r \gg n_d$. Due to this over parameterization and that (13) regards the elements of $\underline{\mathbf{H}}^{\text{inv}}$ as being independent, the phenomenon of over fitting is expected which means that the minimization of (14) does not generally imply good performance, i.e. small (15). Such a problem with more parameters than degrees of freedom is called *ill-posed*.

The solution of ill-posed problems was first studied by Tikhonov et al. [8] who found that the phenomenon of over-fitting can be mitigated by introducing a so-called *regularization functional* $\mathcal{P}(\underline{\mathbf{H}}^{\text{inv}}): \mathbb{R}^{n \times nr} \mapsto \mathbb{R}_+$ into the optimization problem (14) which will penalize those $\underline{\mathbf{H}}^{\text{inv}}$ which are least preferred. Now it is required that $\mathcal{P}(\cdot)$ be

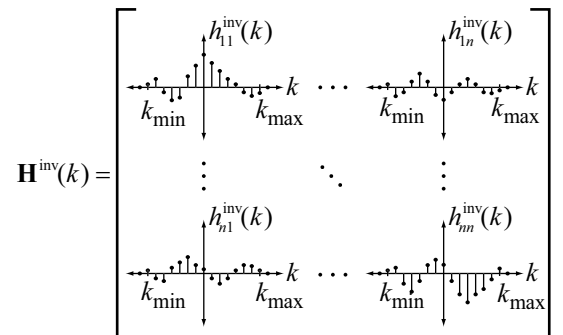


Figure 6. Inverse Impulse Response.

positive semi-definite and is a super set of the null space of $\mathcal{J}(\cdot)$ in (14). With these two conditions met, it may be chosen to convey a preference for a particular structure of \mathbf{H}^{inv} . Thus the minimization problem now has two objectives which must be mutually weighted with the parameter γ as

$$\underset{\mathbf{H}^{\text{inv}}}{\text{minimize:}} \quad \gamma \mathcal{P}(\mathbf{H}^{\text{inv}}) + \mathcal{J}(\mathbf{H}^{\text{inv}}).$$

Commonly the regularization functional is chosen to be of the following quadratic form

$$\mathcal{P}_{\mathbf{Q}}(\mathbf{H}^{\text{inv}}) = \frac{1}{2} \text{vec}(\mathbf{H}^{\text{inv}})^T \mathbf{Q} \text{vec}(\mathbf{H}^{\text{inv}}) \quad (16)$$

where $\text{vec}(\mathbf{A}) : \mathbb{R}^{m \times n} \mapsto \mathbb{R}^{mn}$ vectorizes its argument for some $\mathbf{A} \in \mathbb{R}^{m \times n}$ by stacking its columns and $\mathbf{Q} = \mathbf{Q}^T \in \mathbb{R}^{n^2 r \times n^2 r}$ is a positive semi-definite symmetric matrix. The regularized solution then becomes

$$\hat{\mathbf{H}}^{\text{inv}T} = \text{vec}^{-1} \left(\left(\mathbf{I}_n \otimes \Phi_r^T \Phi_r + \gamma \mathbf{Q} \right)^{-1} \left(\mathbf{I}_n \otimes \Phi_r \right) \text{vec}(\mathbf{N}) \right) \quad (17)$$

where \otimes denotes the *Kronecker product* of two matrices and $\text{vec}^{-1}(\cdot)$ reverses the effects of $\text{vec}(\cdot)$. Now we note if $\mathbf{Q} = \mathbf{I}$, then (17) is known as *ridge regression* and expresses a preference for a *minimum norm* solution. In the case of time-domain modeling there are other more useful choices for \mathbf{Q} as will be developed next.

Time-Domain Regularization – As mentioned, the matrix \mathbf{Q} may be chosen to express a preference/penalty for certain types of impulse responses. This section describes how to choose \mathbf{Q} to express preferred time-domain behavior of \mathbf{H}^{inv} . Without loss of generality consider the SISO (i.e. $n=1$) system with inverse impulse response $h^{\text{inv}}(k)$ and where $\mathbf{H}^{\text{inv}T} = \mathbf{h}^{\text{inv}} \in \mathbb{R}^r$

is a column vector $\left[h^{\text{inv}}(k_{\min}) \quad \dots \quad h^{\text{inv}}(k_{\max}) \right]^T$ which extends forward and backward in time. Due to this acausality, it is expected that $\lim_{k \rightarrow \pm\infty} h^{\text{inv}}(k) = 0$. If k_{\max}

roughly corresponds to the settling time of the system, then for exponential decay it is reasonable to expect that $|h^{\text{inv}}(k)| \leq e(k) \triangleq \alpha \exp\left(\frac{-|k|}{k_c}\right)$ for some α and k_c (see Figure 7). Then if the expected settling behavior is such that $|h^{\text{inv}}(k_{\max})| \approx \mu |h^{\text{inv}}(0)|$ where $0 < \mu \ll 1$ then a

regularization functional $\mathcal{P}_k(\mathbf{h}^{\text{inv}}) = \frac{1}{2} \mathbf{h}^{\text{inv}T} \mathbf{h}^{\text{inv}}$ would unfairly penalize those values for which $k \sim 0$ and will tend to equalize all values of $h^{\text{inv}}(k)$. If instead the values of $h^{\text{inv}}(k)$ were scaled with the envelope $e(k)$ then the settling preference would be properly

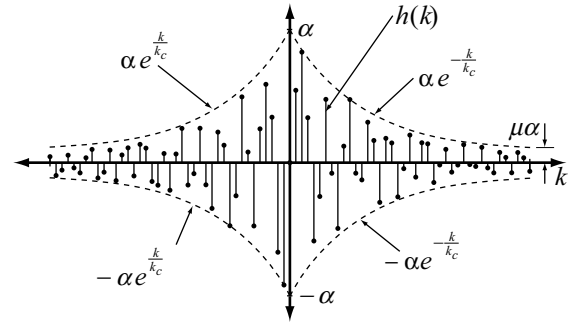


Figure 7. Decaying Impulse response.

expressed. The regularization functional is then defined as

$$\mathcal{P}_k(h^{\text{inv}}(\cdot)) = \frac{1}{2} \sum_{k=k_{\min}}^{k_{\max}} \left(\frac{h^{\text{inv}}(k)}{e(k)} \right)^2 = \mathbf{h}^{\text{inv}T} \mathbf{Q}_k \mathbf{h}^{\text{inv}} \quad (18)$$

where $[\mathbf{Q}_k]_{ij} \triangleq \frac{\delta_{ij}}{e^2(i-k_{\min}+1)} = \delta_{ij} \exp\left(\frac{2|i-k_{\min}+1|}{k_c}\right)$. Then by choosing k_c (which can be thought of as a time constant), the preferred settling behavior of $h(k)$ may be expressed via $\mathcal{P}_k(\cdot)$.

Frequency-Domain Regularization – Similarly, preferences for the frequency-domain behavior of $h(k)$ (we drop the super-script $(\cdot)^{\text{inv}}$ for ease of notation) may be expressed using a regularization functional. First observe that $h(k)$ is a discrete-time aperiodic signal which uses the following Fourier transform pair

$$\begin{aligned} \underline{H}(\theta) &= \mathcal{F}\{h(k)\} \triangleq \sum_{k=-\infty}^{\infty} h(k) e^{-j\theta k} \\ h(k) &= \mathcal{F}^{-1}\{\underline{H}(\theta)\} \triangleq \frac{1}{2\pi} \int_{-\pi}^{\pi} \underline{H}(\theta) e^{j\theta k} d\theta \end{aligned}$$

where $\mathbf{j} \triangleq \sqrt{-1}$ and $\theta \in [-\pi, \pi)$ corresponds to angular frequency such that an unsampled frequency may be obtained as $f = \frac{\theta}{2\pi} f_s$ where $f_s = \frac{1}{T_s}$. To penalize $h(k)$

in the frequency-domain, let $\underline{W}(\theta) : [-\pi, \pi) \mapsto \mathbb{R}_+$ be a positive symmetric weighting function which ascribes a penalty to particular values of $\underline{H}(\theta)$ for every θ . A frequency-domain regularization functional may then be defined as

$$\mathcal{P}_{\theta}(\underline{H}(\cdot)) = \frac{1}{2} \frac{1}{2\pi} \int_{-\pi}^{\pi} |\underline{W}(\theta) \underline{H}(\theta)|^2 d\theta \quad (19)$$

which is expressed in terms of $\underline{H}(\theta) = \mathcal{F}\{h(k)\}$ which is not typically available. Using Parseval's Theorem (19) may be converted to the time-domain as

$$\mathcal{P}_\theta(h(\cdot)) = \frac{1}{2} \sum_{i=k_{\min}}^{k_{\max}} \sum_{j=k_{\min}}^{k_{\max}} h(i)h(j) \sum_{k=-\infty}^{\infty} w(k)w(k+i-j)$$

where $w(k) = \mathcal{F}^{-1}\{\underline{W}(\theta)\}$ has infinite extent (i.e. $k \in (-\infty, \infty)$) but does not have to be calculated explicitly.

Let $[\mathbf{Q}_f]_{ij} = \sum_{k=-\infty}^{\infty} w(k)w(k+i-j)$, then it may be shown that $\sum_{k=-\infty}^{\infty} w(k)w(k+i-j) = \mathcal{F}^{-1}\{\underline{W}^2(\theta)\}(i-j)$ then

$$\mathcal{P}_\theta(h(\cdot)) = \frac{1}{2} \mathbf{h}^T \mathbf{Q}_\theta \mathbf{h}$$

where \mathbf{Q}_θ is symmetric and positive definite and may be determined if $\mathcal{F}^{-1}\{\underline{W}^2(\theta)\}$ can be calculated. A typical example of this technique is when $h(k)$ should be limited to the band of frequencies $\theta_{\text{low}} \leq \theta \leq \theta_{\text{up}}$. In this case

$$\underline{W}(\theta) = \begin{cases} 0 & \theta_{\text{low}} \leq \theta \leq \theta_{\text{up}}, \\ 1 & \text{otherwise} \end{cases}$$

then it is easily shown that

$$[\mathbf{Q}_\theta]_{ij} = \delta(i-j) - \frac{\sin(\theta_{\text{up}}(i-j)) - \sin(\theta_{\text{low}}(i-j))}{\pi(i-j)}$$

for $i \neq j$ and $[\mathbf{Q}_\theta]_{ii} = 1 - \frac{\theta_{\text{up}} - \theta_{\text{low}}}{\pi}$ for $i = j$.

Combined Regularization – These two regularization methods are often used together. They may then be combined as

$$\mathbf{Q} = a\mathbf{Q}_k + b\mathbf{Q}_\theta$$

where if $a, b \geq 0$ then \mathbf{Q} is then positive semi-definite.

NONLINEAR MODELING

Once the linear portion of the inverse model is learned, then the residues become the nonlinear part of the inverse, therefore

$$\mathbf{n}_{\text{nonlin}}(k) = \mathbf{n}(k) - \hat{\mathbf{H}}^{\text{inv}} \underline{\boldsymbol{\phi}}_{\mathbf{r}}(k)$$

and the nonlinear modeling task consists of learning a relationship $\psi: \mathbb{R}^{nr} \mapsto \mathbb{R}^n$ such that

$\psi(\underline{\boldsymbol{\phi}}_{\mathbf{r}}(k)) = \mathbf{n}_{\text{nonlin}}(k) + \mathbf{e}(k)$. Because a nonparametric technique was used for the linear portion of the model, it is appropriate to use a nonparametric technique for the nonlinear portion as well. The data set

$$\left\{ \left(\underline{\boldsymbol{\phi}}_{\mathbf{r}}(k), \mathbf{n}_{\text{nonlin}}(k) \right) \right\}_{k=1}^{\ell} \quad (20)$$

is available with which to train the estimator.

CONSIDERATIONS – Given the desire to find a nonparametric model $\psi(\cdot)$ a suitable approach must be chosen. Several techniques are available to estimate $\psi(\cdot)$. The final selection will be based on the following considerations.

Capacity Control – When one seeks to learn a general mapping $\psi(\cdot)$, all nonparametric methods use a particular fixed structure which is parameterized by $\lambda \in \mathbb{R}^n$ as $\psi(\cdot) = \psi(\cdot; \lambda)$ such that the following optimization problem is solved

$$\underset{\lambda}{\text{minimize}}: \mathcal{J}(\lambda) \triangleq \frac{1}{\ell} \sum_{k=1}^{\ell} L(\mathbf{n}_{\text{nonlin}}(k), \psi(\underline{\boldsymbol{\phi}}_{\mathbf{r}}(k); \lambda)) \quad (21)$$

given a loss function $L(\cdot, \cdot): \mathbb{R}^n \times \mathbb{R}^n \mapsto \mathbb{R}_+$ which generates a penalty for $\psi(\underline{\boldsymbol{\phi}}_{\mathbf{r}}(k); \lambda) \neq \mathbf{n}_{\text{nonlin}}(k)$. It is widely known that the ability to minimize (21) over a training set (20) is dependent on the number of free parameters λ , the structure of $\psi(\cdot; \lambda)$, the inherent complexity of the process which generated the training data (20), and the size of the training set ℓ . Given these concerns it is important to choose $\psi(\cdot; \lambda)$ to avoid the phenomenon of *over fitting* defined as

$$\mathbb{E} \left[L(\mathbf{n}_{\text{nonlin}}(k), \psi(\underline{\boldsymbol{\phi}}_{\mathbf{r}}(k); \lambda_o)) \right] \gg \mathcal{J}(\lambda_o)$$

where λ_o is the optimum obtained in (21). Vladimir Vapnik [9] formalized the notion of “freedom to fit” by defining the notion of *capacity* of $\psi(\cdot; \lambda)$ to fit a set of data. This capacity is theoretically quantifiable using the *VC-dimension*, $\hat{\kappa}$. The phenomenon of over-fitting is then to be expected for $\hat{\kappa} \gtrsim \ell$. It is desirable then to have an estimator with a low VC-dimension. Generally one should expect reasonable performance for an estimator for which $\ell \gtrsim 20\hat{\kappa}$.

The “Curse of Dimensionality” – Due to the nature of nonlinear relationships, many more training samples are required to learn a nonlinear relationship than a linear one. In general, to learn a mapping $\psi: \mathcal{D} \mapsto \mathbb{R}^n$, it is necessary to observe its behavior in all “regions” of the bounded domain $\mathcal{D} \subset \mathbb{R}^d$. The domain \mathcal{D} must then be decomposed into a set of regions Ω_i in which its behavior must be observed. To properly estimate the mapping, each Ω_i must be sufficiently small such that a sample $\mathbf{x} \in \Omega_i$ contained therein represents all of Ω_i and the set $\cup_i \Omega_i$ must *cover* \mathcal{D} . With a vector-valued domain, the number of regions necessary to decompose the domain is exponential in the dimension d of the domain. So as the dimension of the input space increases, it becomes increasingly difficult to obtain sufficient samples to *fill* \mathcal{D} . This is called the “curse of dimensionality”. The reader is referred to Figure 8. This

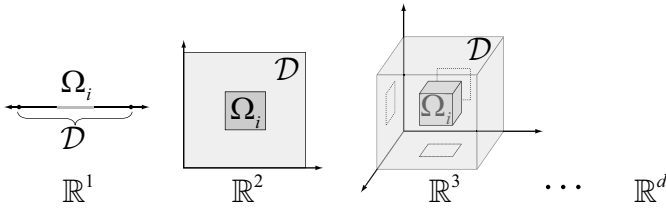


Figure 8. The curse of dimensionality.

reality is a fundamental limitation of non-linear approaches. It motivates the user to limit the dimension of their input space as much as possible and limit the extent of the domain to the smallest possible set.

Available Approaches – Given the problem of learning a general mapping many approaches are available. Methods which have been studied in the literature include artificial neural networks [1], Takagi-Sugeno fuzzy logic, wavelets, splines, etc. Recently a new class of methods called *kernel methods* has been shown to have some advantages over these other methods. By far the most prominent kernel methods to date are the support vector machines (SVM). Their desirable features include:

1. They *generalize* well.
2. They are based on *linear* mathematics.
3. They result in a *global* optimum.
4. They are solved using *quadratic programming* techniques.

The support vector machine will be used to learn the mapping $\psi : \mathbb{R}^{n'} \mapsto \mathbb{R}^n$ on the set given in (20).

SUPPORT VECTOR MACHINE – The support vector machine is a recently developed method for solving nonlinear classification and regression problems (see Cristianini et al. [4]). It was invented by Vapnik and extended by many others. The following two sections present a synopsis of the SVM regression problem for the *scalar-valued* and *vector-valued* cases.

Scalar-Valued Support Vector Regression – Given a general mapping $f : \mathbb{R}^m \mapsto \mathbb{R}$ and the training set $\{(\mathbf{x}_i, y_i)\}_{i=1}^{\ell}$ the SVM seeks to find an estimator $\hat{y}_i = f(\mathbf{x}_i)$ which will perform well on the training set and is expected to perform well in use. The SVM estimator takes the following form

$$\hat{y}(\mathbf{x}) = \langle \mathbf{w}, \boldsymbol{\varphi}(\mathbf{x}) \rangle + b \quad (22)$$

which is linear in the mapped input vector $\boldsymbol{\varphi}(\mathbf{x}_i)$ and has free parameters \mathbf{w} (the weights) and b (the bias). The mapping $\boldsymbol{\varphi} : \mathbb{R}^n \mapsto \mathbb{R}^V$ takes any vector from the *input space* \mathbb{R}^n to a higher-dimensional *feature space* \mathbb{R}^V , that is $V \gg n$. To determine the parameters \mathbf{w} and b which are optimal, a loss function is necessary. In the standard SVM formulation,

$$L(y_i, \hat{y}_i) = |y_i - \hat{y}_i|_{\varepsilon}$$

where $|\cdot|_{\varepsilon}$ is called the ε -insensitive loss function which is defined as $|e|_{\varepsilon} \triangleq \max(0, |e| - \varepsilon)$ and is illustrated in Figure 9. The optimum estimator (22) is then given by

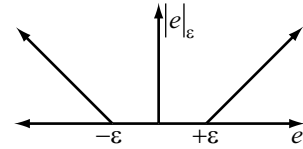


Figure 9. ε -insensitive loss function.

the weight and bias which minimizes $\mathcal{J}(\mathbf{w}, b) = \sum_{i=1}^{\ell} |y_i - \hat{y}_i|_{\varepsilon}$. It is expected that $V > \ell$ implying that the optimum \mathbf{w} and b are not unique. Vapnik has shown that small $\|\mathbf{w}\|$ usually generalize better than large $\|\mathbf{w}\|$ (that is “flatter” models generally predict better). As such, the SVM method employs the regularization functional $\mathcal{P}(\mathbf{w}) \triangleq \frac{1}{2} \|\mathbf{w}\|^2$ yielding the so called *primal* optimization problem

$$[P] \quad \underset{\mathbf{w}, b}{\text{minimize}}: \frac{1}{2} \|\mathbf{w}\|^2 + C \sum_{i=1}^{\ell} |y_i - \hat{y}_i|_{\varepsilon}$$

where \hat{y}_i is defined in (22). Because of the potentially high dimension V of the feature space, the problem is recast into dual form (see Bazaraa et al. [2]) as

$$[D] \quad \underset{\{\beta_i\}_{i=1}^{\ell}}{\text{maximize}}: -\frac{1}{2} \sum_{i,j=1}^{\ell} \beta_i \beta_j k(\mathbf{x}_i, \mathbf{x}_j) + \sum_{i=1}^{\ell} y_i \beta_i - \varepsilon \sum_{i=1}^{\ell} |\beta_i| \quad (23)$$

$$\text{such that } \sum_{i=1}^{\ell} \beta_i = 0 \quad \text{and} \quad |\beta_i| \leq C$$

where $k(\mathbf{x}_i, \mathbf{x}_j) \triangleq \langle \boldsymbol{\varphi}(\mathbf{x}_i), \boldsymbol{\varphi}(\mathbf{x}_j) \rangle$ is the so-called *kernel function* which defines an inner product in feature space. The weight vector in the dual variables β_i becomes $\mathbf{w} = \sum_{i=1}^{\ell} \beta_i \boldsymbol{\varphi}(\mathbf{x}_i)$ and the dual form of the estimator then becomes,

$$\hat{y}(\mathbf{x}) = \sum_{i=1}^{\ell} \beta_i k(\mathbf{x}_i, \mathbf{x}) + b. \quad (24)$$

Notice that both the optimization problem (23) and the estimator (24) are expressed in terms of the kernel function $k(\cdot, \cdot)$ only, not the mapping $\boldsymbol{\varphi}(\cdot)$. Mercer [7] showed that a function $k(\cdot, \cdot)$ which satisfies

$$\int_{\mathcal{X} \times \mathcal{X}} g(\mathbf{x}) k(\mathbf{x}, \mathbf{y}) g(\mathbf{y}) d\mathbf{x} d\mathbf{y} > 0, \quad \forall g(\cdot) \in L^2(\mathcal{X})$$

for $\mathcal{X} \triangleq \text{dom}(g(\cdot))$ implicitly defines the mapping $\boldsymbol{\varphi}(\cdot)$, and guarantees that it is an inner-product space. Such a kernel is called a *Mercer kernel*.

The solution to (23) is typically sparse so let $\mathcal{I}_s \triangleq \{i: \beta_i \neq 0\}$ be the index set of non-zero dual variables. Then the so-called *support vectors* are defined by $\{\mathbf{x}_i\}_{i \in \mathcal{I}_s}$. This sparseness property of the SVM allows them to adjust their capacity to the complexity of the training data. This allows them to generalize well.

Vector-Valued Support Vector Regression – A generalization of scalar-valued SVR is the vector-valued SVR which is designed to learn a mapping of the form $\mathbf{f}: \mathbb{R}^m \mapsto \mathbb{R}^d$ given a training set $\{(\mathbf{x}_i, \mathbf{y}_i)\}_{i=1}^{\ell}$. In VV-SVR (see Brudnak [3] for full development) the estimator takes the general form

$$\hat{\mathbf{y}}(\mathbf{x}) = \mathbf{W}\boldsymbol{\varphi}(\mathbf{x}) + \mathbf{b}$$

where $\mathbf{W} \in \mathbb{R}^{d \times v}$ is a weight matrix and $\mathbf{b} \in \mathbb{R}^d$ is the bias vector. The vector-valued loss function is defined as

$$L(\mathbf{y}_i, \hat{\mathbf{y}}_i) = \left\| \mathbf{y}_i - \hat{\mathbf{y}}_i \right\|_p \Big|_{\mathcal{E}}$$

where $1 \leq p \leq \infty$ represents the p -norm of the error. The primal optimization problem is

$$\boxed{P} \quad \underset{\mathbf{W}, \mathbf{b}}{\text{minimize:}} \quad \frac{1}{2} \|\mathbf{W}\|_F^2 + C \sum_{i=1}^{\ell} \left\| \mathbf{y}_i - \hat{\mathbf{y}}_i \right\|_p \Big|_{\mathcal{E}}$$

which leads to the dual problem

$$\boxed{D} \quad \underset{\{\Gamma_i\}_{i=1}^{\ell}}{\text{maximize:}} \quad -\frac{1}{2} \sum_{i,j=1}^{\ell} \Gamma_i \Gamma_j k(\mathbf{x}_i, \mathbf{x}_j) + \sum_{i=1}^{\ell} \mathbf{y}_i \Gamma_i - \mathcal{E} \sum_{i=1}^{\ell} \|\Gamma_i\|_q$$

$$\text{such that } \sum_{i=1}^{\ell} \Gamma_i = 0 \quad \text{and} \quad \|\Gamma_i\|_q \leq C$$

where $\|\cdot\|_p$ and $\|\cdot\|_q$ are *conjugate* norms (i.e. $\frac{1}{p} + \frac{1}{q} = 1$).

Given that $\mathbf{W} = \sum_{i=1}^{\ell} \Gamma_i \boldsymbol{\varphi}(\mathbf{x}_i)$, the final form of the estimator becomes

$$\hat{\mathbf{y}}(\mathbf{x}) = \sum_{i=1}^{\ell} \Gamma_i k(\mathbf{x}_i, \mathbf{x}) + \mathbf{b}.$$

The index set for the support vectors becomes $\mathcal{I}_s \triangleq \{i: \|\Gamma_i\|_q \neq 0\}$ and the support vectors are defined as $\{\mathbf{x}_i\}_{i \in \mathcal{I}_s}$. This vector valued version is used to learn nonlinear mappings for MIMO systems.

COMPOSITE MODELING

Now two models exist of the inverse of the plant. One is linear; the other is nonlinear. A composite model is created as shown in Figure 3 and Figure 4 by summing the output of the two models. To estimate these models the plant is excited with the random time series $\mathbf{n}(k)$ and

the associated response $\mathbf{r}(k)$ is recorded. From these, the data set $\{(\mathbf{n}(k), \mathbf{r}(k))\}_{k=1}^{\ell}$ is used to learn the inverse impulse response function $\mathbf{H}^{\text{inv}}(\cdot)$ as discussed above. The best linear estimate of the inverse plant is therefore defined as $\hat{\mathbf{H}}^{\text{inv}}(\cdot)$. The predicted input based on the linear model then becomes $\hat{\mathbf{n}}(k) \triangleq \hat{\mathbf{H}}^{\text{inv}}(\cdot) * \mathbf{r}(k)$. The deviations from the linear model may then be estimated as $\mathbf{d}(k) = \mathbf{n}(k) - \hat{\mathbf{n}}(k)$. By hypothesis $\mathbf{d}(k)$ contains information regarding the nonlinear part of the model, therefore the training set $\mathcal{D}_0 \triangleq \{(\boldsymbol{\varphi}_{\mathbf{r}}(k), \mathbf{d}(k))\}_{k=1}^{\ell}$ may be learned as a mapping. The vector-valued support vector machine approach will be used to accomplish this. The estimated mapping will be denoted as $\hat{\psi}_0: \mathbb{R}^{nr} \mapsto \mathbb{R}^n$ and takes the form $\hat{\psi}_0\left(\{\mathbf{r}(k)\}_{k=k_{\min}}^{k_{\max}}\right) \equiv \hat{\psi}_0(\boldsymbol{\varphi}_{\mathbf{r}}(k))$. Once this mapping is learned it may be used to estimate the proper drive which will yield the proper response as follows

$$\hat{\mathbf{c}}(k) \triangleq \hat{\mathbf{H}}^{\text{inv}} \boldsymbol{\varphi}_{\mathbf{a}}(k) + \hat{\psi}_0(\boldsymbol{\varphi}_{\mathbf{a}}(k))$$

where $\boldsymbol{\varphi}_{\mathbf{a}}(k)$ is the vectorized (i.e. indexed by λ) desired response $\mathbf{a}(k)$. So if $\hat{\mathbf{H}}^{\text{inv}}$ and $\hat{\psi}_0(\cdot)$ properly represent the inverse dynamics then $\hat{\mathbf{c}}(k)$ will be a good estimate of the drive and it is expected that the actual rig response will be equal to the desired response, that is

$$\mathbf{f}_{\mathbf{a}}(\hat{\mathbf{c}}(k)) \approx \mathbf{a}(k).$$

If the desired response $\mathbf{a}(k)$ is statistically dissimilar from the SYS-ID excitation response $\mathbf{r}(k)$ then the curse of dimensionality indicates that $\hat{\psi}_0(\cdot)$ will not necessarily be a good model for the inputs $\mathbf{a}(k)$. In such cases the nonlinear mapping may have to be re-learned for plant outputs which are closer to the desired response. The next section discusses a couple of alternative approaches.

THE CONTROL SCHEME

In this section strategies for determining the best estimated drive $\hat{\mathbf{c}}(k)$ are discussed. Typically the first estimate of the drive (called $\hat{\mathbf{c}}_0(k)$) is not the best possible drive by the criteria stated in (8). To achieve the optimum drive, typically a sequence of drives is estimated $\hat{\mathbf{c}}_0(\cdot), \hat{\mathbf{c}}_1(\cdot), \dots, \hat{\mathbf{c}}_f(\cdot)$ until an acceptable level of accuracy is attained. Two alternative strategies are presented here.

PREDICT-CORRECT – This method requires a linearization of the estimated inverse plant. Let

$$\hat{\mathbf{f}}^{\text{inv}}(\underline{\boldsymbol{\varphi}}_a(k)) \triangleq \hat{\mathbf{H}}^{\text{inv}} \underline{\boldsymbol{\varphi}}_a(k) + \hat{\boldsymbol{\psi}}_0(\underline{\boldsymbol{\varphi}}_a(k))$$

then

$$\mathbf{J}^{\text{inv}}(\underline{\boldsymbol{\varphi}}_a) \triangleq \frac{\delta}{\delta \underline{\boldsymbol{\varphi}}_a} \hat{\mathbf{f}}^{\text{inv}}(\underline{\boldsymbol{\varphi}}_a) = \hat{\mathbf{H}}^{\text{inv}} + \frac{\delta}{\delta \underline{\boldsymbol{\varphi}}_a} \hat{\boldsymbol{\psi}}_0(\underline{\boldsymbol{\varphi}}_a)$$

where $\mathbf{J}^{\text{inv}}(\underline{\boldsymbol{\varphi}}_a)$ is the Jacobian of $\hat{\mathbf{f}}^{\text{inv}}(\underline{\boldsymbol{\varphi}}_a)$. The rig response which is generated by the drive $\hat{\mathbf{c}}_i(\cdot)$ is $\tilde{\mathbf{a}}_i(\cdot)$ and the associated error is given by $\mathbf{e}_i(\cdot)$. The Jacobian may then be used to estimate a new drive given by

$$\hat{\mathbf{c}}_{i+1}(\cdot) = \hat{\mathbf{c}}_i(\cdot) + \mathbf{w}_{i+1} \circ (\mathbf{J}^{\text{inv}}(\underline{\boldsymbol{\varphi}}_a) \mathbf{e}_i(\cdot))$$

where $\mathbf{w}_{i+1} \in [0,1]^n$ is a weight vector. Because of the nature of the method, it is called *predict-correct*. First, note that this method reduces to the linear method in Equation (7) when $\hat{\boldsymbol{\psi}}_0(\underline{\boldsymbol{\varphi}}_a) \equiv \mathbf{0}$. Secondly, this method is expected to work well if $\hat{\boldsymbol{\psi}}_0(\underline{\boldsymbol{\varphi}}_a)$ is a very good approximation of the nonlinear portion of the inverse model's derivative. It is not expected that this will be the case. For this reason the approach presented in the following section is preferred.

OBSERVE-ADAPT – Another method which does not require the calculation or estimation of a derivative is the method called *observe-adapt*. In this method, the linear part $\hat{\mathbf{H}}^{\text{inv}}$ is held fixed and the nonlinear part of the model is adapted to new plant observations. Given the initial nonlinear inverse model $\hat{\boldsymbol{\psi}}_0(\underline{\boldsymbol{\varphi}}_a)$, which was trained on \mathcal{D}_0 , it is used to calculate an initial drive estimate $\hat{\mathbf{c}}_0(k)$ which produces an associated rig response $\tilde{\mathbf{a}}_0(\cdot)$. It is expected that this response will not be optimal, however, by hypothesis, it should be closer to desired response $\mathbf{a}(k)$ than to the original random excitation response of $\mathbf{r}(k)$. In this case then the associated deviation from the linear model may be estimated as $\mathbf{d}_0(k) = \hat{\mathbf{c}}_0(k) - \hat{\mathbf{H}}^{\text{inv}} \tilde{\mathbf{a}}_0(k)$ and if the desired data is indexed by $(1, \dots, L)$ an augmented training set may then be developed as $\mathcal{D}_1 \triangleq \mathcal{D}_0 \cup \left\{ \left(\underline{\boldsymbol{\varphi}}_{\tilde{\mathbf{a}}_0}(k), \mathbf{d}_0(k) \right) \right\}_{k=1}^L$. The set \mathcal{D}_1 may then be used to estimate a new mapping such that $\boldsymbol{\psi}_1(\cdot) \models \mathcal{D}_1$ where the symbol \models denotes that $\boldsymbol{\psi}_1(\cdot)$ *models* or *generalizes* the set \mathcal{D}_1 . This new nonlinear model may then be used to produce a better drive as $\hat{\mathbf{c}}_1(k) \triangleq \hat{\mathbf{H}}^{\text{inv}} \underline{\boldsymbol{\varphi}}_a(k) + \hat{\boldsymbol{\psi}}_1(\underline{\boldsymbol{\varphi}}_a(k))$. This process may then be generalized to the following algorithm.

1. **Given:** The estimated drive $\hat{\mathbf{c}}_i(k)$, the corresponding response $\underline{\boldsymbol{\varphi}}_{\tilde{\mathbf{a}}_i}(k)$, the linear model $\hat{\mathbf{H}}^{\text{inv}}$ and the training set \mathcal{D}_i .

2. **If** $\mathbf{m}_i = \frac{\text{RMS}_k(\mathbf{a}(k) - \tilde{\mathbf{a}}_i(k))}{\text{RMS}_k(\mathbf{a}(k))} \leq \tau$ for some threshold τ **then stop**.
3. **Let** $\mathbf{d}_i(k) = \hat{\mathbf{c}}_i(k) - \hat{\mathbf{H}}^{\text{inv}} \underline{\boldsymbol{\varphi}}_{\tilde{\mathbf{a}}_i}(k)$.
4. **Form** $\mathcal{D}_{i+1} \triangleq \mathcal{D}_i \cup \left\{ \left(\underline{\boldsymbol{\varphi}}_{\tilde{\mathbf{a}}_i}(k), \mathbf{d}_i(k) \right) \right\}_{k=1}^L$.
5. **Train** $\boldsymbol{\psi}_{i+1}(\cdot)$ such that $\boldsymbol{\psi}_{i+1}(\cdot) \models \mathcal{D}_{i+1}$.
6. **Estimate** the next drive $\hat{\mathbf{c}}_{i+1}(k) \triangleq \hat{\mathbf{H}}^{\text{inv}} \underline{\boldsymbol{\varphi}}_a(k) + \hat{\boldsymbol{\psi}}_{i+1}(\underline{\boldsymbol{\varphi}}_a(k))$.
7. **Play** $\hat{\mathbf{c}}_{i+1}(k)$ into the rig and **record** the response $\tilde{\mathbf{a}}_{i+1}(k)$.
8. **Goto** step 2.

In this way, if the sequence of responses continues to get closer to the desired response (i.e. $\mathbf{m}_i > \mathbf{m}_{i+1}$) then the sequence of models ($\boldsymbol{\psi}_0(\cdot), \boldsymbol{\psi}_1(\cdot), \dots, \boldsymbol{\psi}_i(\cdot), \dots$) should converge to the best representation of the nonlinear behavior at the operating point.

EXAMPLE

To demonstrate some of the methods presented, consider a 2x2 system (i.e. $n = 2$) which comprises the rear two tires of a single-axle military trailer (see Figure 10) where the two inputs $c_1(k)$ and $c_2(k)$ are displacement commands to the left and right actuators respectively and the responses $\tilde{a}_1(k)$ and $\tilde{a}_2(k)$ are the associated acceleration responses at the left and right wheel spindles. The control problem is then to develop the proper drive command $\mathbf{c}(k)$ such that the acceleration responses match some a-priori specified response $\mathbf{a}(k)$. In this example the linear SYS-ID portion of the above developed process will be demonstrated.

To begin the system identification process a random noise command $\mathbf{n}(k)$ is generated with which to excite the system. Such excitation commands are typically specified in the frequency-domain as shown in Figure 11. They are then converted to the time-domain such that they are uncorrelated in the time-domain. Because the system is not linear, it is desirable to excite the system at



Figure 10. Military trailer which comprises 2x2 system.

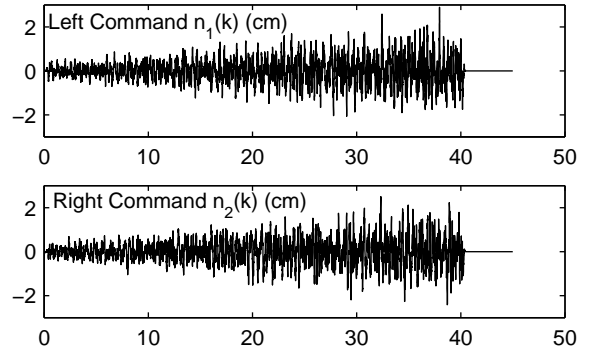
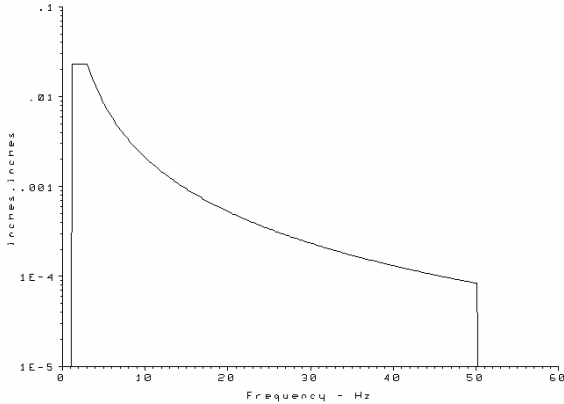


Figure 12. Plot of random excitation $\mathbf{n}(k)$.

all energy levels from mild to severe, the time history is linearly increased in amplitude throughout its duration. In this particular case it was designed to begin at roughly ± 0.5 cm and progressively increase to roughly ± 2.5 cm. The generated time histories are shown in Figure 12. This time history was played into the simulator and the associated response $\mathbf{r}(k)$ was recorded. Both of the input and output were discretized at a sample rate of $f_s = 204.8$ Hz. The techniques of linear time-domain modeling were applied to the recorded inputs and outputs to learn the inverse time-domain model $\hat{\mathbf{H}}^{\text{inv}}(k)$. For reference purposes, the inverse impulse response function was calculated for $k_{\min} = -400$ and $k_{\max} = 400$ which is shown in Figure 13 where the average mean squared error was 0.1209 cm.

The time-domain regularization technique is demonstrated by training on the same information however expressing a preference that $\hat{\mathbf{H}}^{\text{inv}}(k)$ decay to a value of 10% at $k_s = 400$. The estimated impulse response function is shown in Figure 14. In this case the average mean squared error was 0.1218 cm which is very close to the unregularized optimum. It is therefore observed that the performance has degraded by about 0.7% but the model is much different. This is evidence that the original solution in Figure 13 was unstable or the problem was ill-posed.

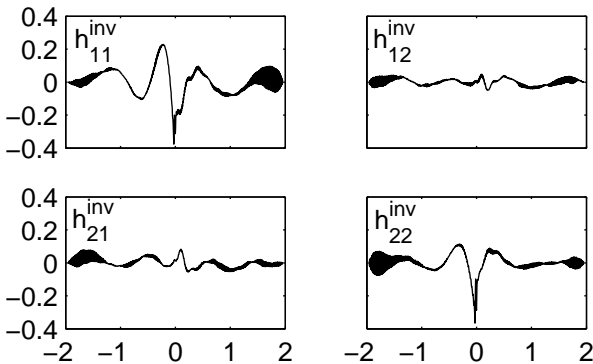


Figure 13. Plot of least squares result of $\hat{\mathbf{H}}^{\text{inv}}(k)$ for unregularized least squares learning ($\gamma = 0$).

The frequency-domain regularization technique is demonstrated by using this technique to penalize those components of $\hat{\mathbf{H}}^{\text{inv}}(k)$ for which $f < 1$ Hz and $f > 50$ Hz. The estimated impulse response is shown in Figure 15. Again in this case the average mean squared error was 0.1210 cm which is very close to the unregularized value of 0.1209 cm which is again evidence of an ill-posed problem.

CONCLUSION

This paper presented an approach to full-vehicle simulator control which accounts for nonlinearities in vehicle/simulator system. To improve on the standard linear methods of Cryer et al. a composite linear and nonlinear approach to inverse system identification was developed. The linear method developed operates in the time-domain and employs regularization to express preferences for model behavior in either the time- or frequency-domain. The nonlinear portion of the model is designed to learn the nonlinear deviations from the linear model and the vector-valued support vector machine is used to learn this deviation. Two approaches are presented which describe how to iteratively improve the drive command estimate which are called predict-correct and observe-adapt. The linear regularized techniques are demonstrated for a 2x2 system.

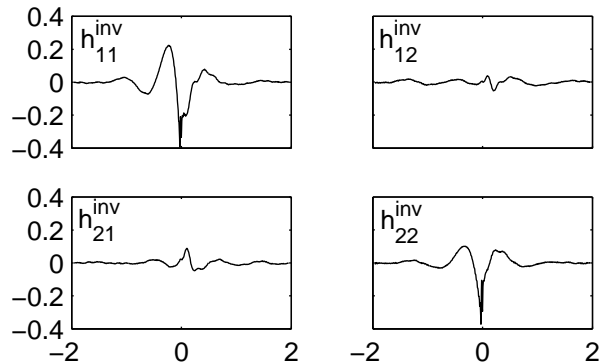


Figure 14. Plot of least squares result of $\hat{\mathbf{H}}^{\text{inv}}(k)$ for time-domain regularization with settling time defined by $\mu = 0.1$, $k_s = 400$ and $\gamma = 1$.

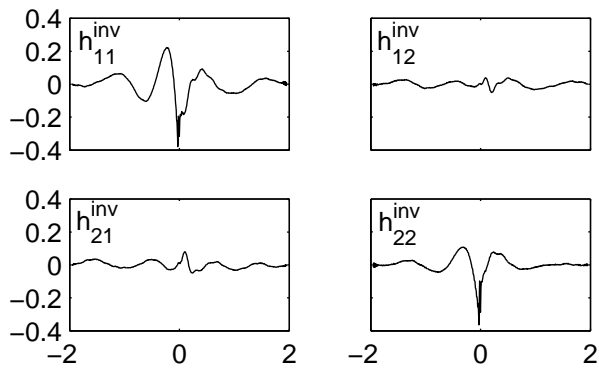


Figure 15. Plot of least squares result of $\hat{\mathbf{H}}^{\text{inv}}(k)$ for frequency-domain regularization with settling time defined by $f_{\text{low}} = 1 \text{ Hz}$, $f_{\text{up}} = 50 \text{ Hz}$ and $\gamma = 1$.

ACKNOWLEDGMENTS

The author would like to acknowledge the U.S. Army Research Development and Engineering Command (RDECOM) and the Tank Automotive Research Development and Engineering Center (TARDEC) ILIR program for funding this work.

REFERENCES

1. Barber, A.J., "Accurate Models for Complex Vehicle Components Using Empirical Methods", Paper 2000-01-1625, Society of Automotive Engineers, 2000.
2. Bazaraa, M.S., Sherali, H.D., Shetty, C.M., *Nonlinear Programming: Theory and Algorithms*, 2nd ed., John Wiley & Sons, New York, 1993.
3. Brudnak, M.J., "Support Vector Methods for the Control of Unknown Nonlinear Systems", Ph.D. dissertation, Oakland University, Rochester, MI, 2005.
4. Cristianini, N., Shawe-Taylor, J., *An Introduction to Support Vector Machines and other kernel-based learning methods*, Cambridge University Press, New York, 2000.
5. Cryer, B.W., Nawrocki, P.E., Lund, R.A., "A Road Simulation System for Heavy Duty Vehicles", Paper 760361, Society of Automotive Engineers, 1976.
6. Fash, J.W., Goode, J.G., Brown, R.G., "Advanced Simulation Testing Capabilities", Paper 921066, Society of Automotive Engineers, 1992.
7. Mercer, J., "Functions of a positive and negative type and their connection with the theory of integral

equations", *Philosophical transactions of the Royal Society, London*, A 209: pp. 415-446, 1909.

8. Tikhonov, A.N., Arsenin, V.Y., *Solutions of Ill-Posed Problems* (English translation by Fritz John), V.H. Winston & Sons, Washington D.C., 1977.
9. Vapnik, V.N. *The Nature of Statistical Learning Theory*, Springer, New York, 1995.
10. Whitmore, A.P., "A Technique for Measuring 'Effective' Road Profiles", Paper 720095, Society of Automotive Engineers, 1972.

CONTACT

Mark J. Brudnak
 U.S. Army RDECOM-TARDEC
 6501 East Eleven Mile Road
 ATTN: AMSRD-TAR-N/157
 Warren, MI 48397-5000
 (586)574-7355
 mark.brudnak@us.army.mil

DEFINITIONS, ACRONYMS, ABBREVIATIONS

ASD	Auto Spectral Density.
CSD	Cross Spectral Density.
DFT	Discrete Fourier Transform.
FFT	Fast Fourier Transform.
FIR	Finite Impulse Response.
FRF	Frequency Response Function.
FVTR	Full Vehicle Test Rig.
HMMWV	High-Mobility Multipurpose Wheeled Vehicle.
MIMO	Multiple Input Multiple Output.
RDECOM	Research Development and Engineering Command.
RMS	Root Mean Squared.
SISO	Single Input Single Output.
SVM	Support Vector Machine.
SVR	Support Vector Regression.
SYS-ID	System Identification.
TARDEC	Tank Automotive Research Development and Engineering Command.